Spatially Localized Unstable Periodic Orbits

Scott M. Zoldi[*][†] and Henry S. Greenside[*]

Department of Physics

Duke University, Durham, NC 27708-0305

(April 2, 1997)

Abstract

Using an innovative damped-Newton method, we report the first calculation of many distinct unstable periodic orbits (UPOs) of a large high-dimensional extensively chaotic partial differential equation. A majority of the UPOs turn out to be spatially localized in that time dependence occurs only on portions of the spatial domain. With a particular weighting of 127 UPOs, the Lyapunov fractal dimension $D = 8.8$ can be estimated with a relative error of 2%. We discuss the implications of these spatially localized UPOs for understanding and controlling spatiotemporal chaos.

47.27.Cn, 05.45.+b, 05.70.Ln, 82.40.Bj

Much recent research on sustained nonequilibrium systems has concerned using unstable periodic orbits (UPOs) to characterize and to control chaos [1–5]. The starting point for this research has been the observation that a dense set of unstable periodic orbits (UPOs) is associated with a strange attractor. [6]. For low-dimensional chaos with a symbolic dynamics (a unique labeling of the UPOs in the dense set [6]), researchers have shown that knowledge of a small number of UPOs can be used to improve forecasting [7] and to estimate dynamical invariants of the strange attractor such as its fractal dimensions and Lyapunov exponents [1]. In some low-dimensional chaotic experimental systems, enough UPOs have been determined from empirical data to apply this formalism successfully [3]. An exciting related advance has been the discovery that these low-dimensional chaotic systems can be controlled by stabilizing particular members of the dense set of UPOs with weak time-dependent perturbations of a system parameter [8].

An important question is whether the above results generalize and remain useful for high-dimensional dynamical systems, especially for large nonequilibrium systems that are extensively chaotic [9, 10]. We are particularly interested in two potential applications. One is to characterize extensive chaos in terms of some finite number of UPOs [2]. Large nonequilibrium chaotic systems are difficult to analyze because of long transient times (which, in some cases, increase exponentially with system size [11]) and also because it is often not known in advance how long a system should be observed in a non-transient regime to obtain good statistics. An attractive feature of UPOs associated with a strange attractor is that *they can be computed within a finite time interval* and so their analysis replaces difficult questions of transients and observation times with questions of mathematical and numerical convergence, e.g., the number of UPOs needed to approximate the invariant measure of an attractor to some desired accuracy and whether sufficiently many UPOs can be calculated numerically. A second potential application is to improve control of extensively chaotic systems. If the magnitude of a control perturbation is to remain small as a chaotic system becomes large, the system parameter will need to be varied at spatially distributed control points [12]. An improved understanding of the spatial structure of UPOs, of the distribu-

tion of their periods T, and of their stability should aid the development of high-dimensional spatiotemporal control algorithms by suggesting the number and location of control points for a particular UPO and for a particular system parameter.

In this Letter, we take a significant step towards understanding the relation of the dense set of UPOs to high-dimensional spatiotemporal chaos by reporting the first calculation of many (over 100) distinct UPOs for a high-dimensional ($D = 8.8$) driven-dissipative system partial differential equation (pde) in an extensively chaotic regime [13]. This calculation represents two achievements. One is numerical, that a simple modification of a Newton algorithm by the addition of damping [14] greatly increases the likelihood of convergence and so makes practical the computation of many UPOs from the nonlinear equations that they satisfy. The second achievement is several discoveries in nonequilibrium physics made possible by this numerical method: that over 100 distinct UPOs can be calculated in a large chaotic pde and therefore their properties can be studied for the first time; that most of these UPOs turn out to be spatially localized (as discussed below); that about 100 UPOs are already sufficient to estimate the fractal dimension of the high-dimensional attractor to two significant digits; and that certain mean quantities such as a time-averaged spatial pattern can be estimated from a knowledge of the UPOs.

Especially interesting is the result that most of the UPOs have dynamics that are spatially localized in that the variance of temporal fluctuations is substantial only on portions of the spatial domain (see Figs. 1 and 2 below). We speculate that this will be a general feature of UPOs for extensively chaotic systems. This localization, in fact, helps to explain how the spatiotemporal disorder of an extensively chaotic system (which can be interpreted as many small dynamically-independent subsystems [10]) can be consistent with the global spatiotemporal coherence of each UPO in the dense set. The temporal disorder can be understood as an irregular wandering of a chaotic orbit near many UPOs (the case for low-dimensional chaos) while the spatial disorder can now be better understood as a complicated weighting of localized spatially-irregular dynamics associated with the UPOs. The spatially localized dynamics also has implications for distributed control algorithms since control

points placed in the weakly time-independent spatial regions of a particular UPO will likely not aid in stabilizing that UPO. It is then important to know the spatial structure of various UPOs before attempting to control them.

Our calculations were carried out for one of the simplest models of extensive chaos, the one-dimensional Kuramoto-Sivashinsky (KS) equation [9]

$$\partial_t u = -u\,\partial_x u - \partial_x^2 u - \partial_x^4 u, \qquad x \in [0, L], \tag{1}$$

for a field $u(t, x)$ that lives on an interval of length L and that satisfies "rigid" boundary conditions $u = \partial_x u = 0$ at $x = 0$ and $x = L$. For system sizes $L \geq 50$, Manneville has shown that typical initial conditions evolve towards a chaotic attractor that is extensive in that the Lyapunov fractal dimension D increases linearly with L [15]. In our calculations, we chose a fixed length $L = 50$ and spatial resolution $\triangle x = 0.5$ for which the Lyapunov fractal dimension was $D = 8.8$ and there were 4 positive, 1 zero, and 94 negative Lyapunov exponents [16]. The system size $L = 50$ was just large enough to be in the extensively chaotic regime and yet small enough that the numerical calculations were manageable with available resources and algorithms. The reason for emphasizing the extensively chaotic regime was that certain details of the spatiotemporal chaos and of the UPOs could then be expected to be insensitive to the value of the system length L.

UPOs of Eq. (1) were calculated numerically by using a damped-Newton method [14] with simple shooting [17, pages 120-122] to solve a set of nonlinear equations $\mathbf{F}(\mathbf{X}) = \mathbf{0}$ for unknowns $\mathbf{X} = (T, \mathbf{U}_0)$ which we define as follows. Given a uniformly spaced mesh $x_i = i\triangle x$ on the interval $[0, L]$ with spatial resolution $\triangle x = L/(N+1)$, we denote the field value at the ith mesh point at time t by $u_i(t) = u(x_i, t)$ for $i = 0, \cdots, N + 1$. Then the $(N+1)$-dimensional vector of unknowns $\mathbf{X}$ consists of the UPO's period T and of a N-dimensional point $\mathbf{U}_0 = (u_1(0), \cdots, u_N(0))$ that lies on the UPO. The values $u_0 = u(t, 0)$ and $u_{N+1} = u(t, L)$ are zero by the boundary conditions and do not need to be solved for.

The corresponding $(N+1)$-dimensional nonlinear equations $\mathbf{F}(\mathbf{X}) = 0$ for $\mathbf{X}$ are determined by trying to find a closed orbit $\mathbf{U}_t$ of duration T starting from $\mathbf{U}_0$, i.e., such

4

that $\mathbf{U}_T - \mathbf{U}_0 = \mathbf{0}$. These nonlinear equations are derived and solved as follows. First, Eq. (1) is reduced to a N-dimensional set of first-order autonomous odes,

$$dU/dt = \mathbf{G}(\mathbf{U}), \qquad \mathbf{U}(0) = \mathbf{U}_0. \tag{2}$$

by replacing the spatial derivatives in Eq. (1) and in the boundary condition $\partial_x u = 0$ with second-order accurate finite-difference approximations. The vector $\mathbf{U}_T$ at time T is then found by numerical integration of Eq. (2). Second, a $N \times N$ matrix $\mathbf{M}_T$ at time T is obtained by integrating the N^2 linear variational equations [17]

$$dM/dt = \mathbf{JM}, \qquad \mathbf{M}(0) = \mathbf{I}, \tag{3}$$

together with Eq. (2), where $\mathbf{J}(t) = \partial \mathbf{G}/\partial \mathbf{U}$ denotes the $N \times N$ Jacobian matrix and $\mathbf{I}$ denotes the $N \times N$ identity matrix. (The matrix $\mathbf{M}(t)$ is the propagator that evolves infinitesimal perturbations from time $t = 0$ to time t.) Given the vector $\mathbf{U}_T$ and matrix $\mathbf{M}_T$, a Newton correction $\delta \mathbf{X} = (\delta T, \delta \mathbf{U})$ for updating the vector $\mathbf{X}$ is found by solving the following 2×2 block matrix equation [17]:

$$\begin{pmatrix} \mathbf{0} & \mathbf{G}(\mathbf{U}_0)^\dagger \\ \mathbf{G}(\mathbf{U}_T) & \mathbf{M}_T - \mathbf{I} \end{pmatrix} \begin{pmatrix} \delta T \\ \delta \mathbf{U} \end{pmatrix} = \begin{pmatrix} \mathbf{0} \\ \mathbf{U}_0 - \mathbf{U}_T \end{pmatrix}, \tag{4}$$

where the symbol $\dagger$ denotes the matrix transpose. A single Newton step is then performed by updating the present values for the unknowns, $\mathbf{X} \to \mathbf{X} + \delta \mathbf{X}$, and such steps are repeated until the residuals and corrections are sufficiently small

$$\|\mathbf{U}_T - \mathbf{U}_0\|_\infty < 10^{-3}\|\mathbf{U}_0\|_\infty, \qquad \text{and} \qquad \|\delta \mathbf{X}\|_\infty < 10^{-3}\|\mathbf{X}_0\|_\infty, \tag{5}$$

in the infinity norm $\|\mathbf{X}\|_\infty = \max_i |X_i|$. Each Newton step requires the time-integration of a set of $N + N^2$ odes over time T plus the solution of the linear equations Eq. (4). For the calculations reported below, we used time-splitting methods for Eqs. (2) and (3) that were first-order accurate in time and second-order accurate in space with a constant time step $\triangle t = 0.005$. Since the block matrix $\mathbf{M}_T - \mathbf{I}$ in Eq. (4) is typically dense, PLU-factorization was used to solve for the correction; the time to carry out the linear algebra was much larger

the time to integrate Eqs. (2) and (3) over a period T. Most UPOs that we calculated were robust to modest changes in spatiotemporal resolution and the Newton convergence criteria.

For high-dimensional Newton methods, it is essential to have a good starting guess $\mathbf{X}_0$ since Newton methods are guaranteed to converge only locally. We initially tried to find a good initial guess $(T, \mathbf{U}_0)$ by searching for approximate recurrences [3, 7] of chaotic time series $\mathbf{U}_i = \mathbf{U}(i \triangle t)$ in the high-dimensional numerical phase space of Eq. (2). This turned out to be impractical, e.g., for $L = 50$, integration times of at least 10^8 time units were needed to find a single approximate recurrence of period $T = 11.6$ within a ball of rather large radius 0.1, $\|\mathbf{U}_T - \mathbf{U}_0\|_\infty < 0.1$ [18]. Further, these approximate recurrences did not turn out to be close to any of the UPOs that we calculated using the more rigorous Newton method [19]. Since these results suggest that no approximate recurrence is close to a UPO of Eq. (1), we then tried to choose an initial state by choosing a positive random number T for the period and an initial vector $\mathbf{U}_0$ from a point on the chaotic attractor. Using this procedure, the convergence criteria Eq. (5) always failed within the specified maximum number of 200 Newton iterations.

Convergence was finally obtained with a *damped*-Newton method [14], in which only a fraction $\alpha \leq 1$ of a Newton correction $\delta \mathbf{X}$ was added to update the unknowns, $\mathbf{X} \rightarrow \mathbf{X} + \alpha \delta \mathbf{X}$. We used a particular damping method known as the Armijo rule [14] which expresses the damping factor in the form $\alpha = 2^{-j}$. During each Newton iteration, successive values of the integer $j = 0, 1, \cdots$ were tested until a value j was found such that the new residual $\|\mathbf{F}(\mathbf{X} + 2^{-j}\delta \mathbf{X})\|$ was smaller by a factor $1 - \alpha/2$ than the previous residual $\|\mathbf{F}(\mathbf{X})\|$ in the Euclidean norm. With the Armijo rule, Newton's method converged with the criteria Eq. (5) for roughly five percent of all initial guesses $(T, \mathbf{U}_0)$ consisting of a positive random number T and some point $\mathbf{U}_0$ on the chaotic attractor. If the damping parameter α fell below the value 2^{-6}, it was more efficient to terminate the Newton iteration and start over with a new guess $(T, \mathbf{U}_0)$. The specific value of $j = 6$ was chosen as a trade off between convergence and computer time, as tiny fractions of the correction can lead to an excessive amount of time spent on a single guess.

We now discuss the properties of the UPOs calculated with the above numerical methods. Using the Armijo rule and the Newton method discussed above, 127 distinct UPOs were found from 5000 guess $\mathbf{X}_0 = (T_0, \mathbf{U}_0)$ [19]. UPOs with periods shorter than 8 could not be found while the Armijo-Newton algorithm failed to converge for UPOs with periods larger than 42, probably because the simple shooting method becomes unstable for periods larger than about this value.

As shown qualitatively in Fig. 1 and more quantitatively in Fig. 2, most of the UPOs are localized in that their time variation is substantial only in isolated portions of the domain. Fig. 1(A) shows a state for which the temporal variation is localized in two small spatial intervals, one of which is adjacent to the right boundary. Fig. 1(B) shows an interior state whose dynamics is localized to a single interval well away from the boundaries. Fig. 1(C) shows an extended UPO in which the temporal variation occurs throughout the spatial domain. The corresponding mean and variance patterns [19] are given in Fig. 2(a)-(f). In Fig. 2(a), (c), and (e), the mean pattern is nonzero throughout the domain which holds for the other 124 UPOs as well. Fig. 2(b) and (d) indicate more clearly the localization of the dynamics, which is evidently uncorrelated with the mean pattern. The variance decreases three to five orders of magnitude outside the regions of substantial variation.

From an explicit knowledge of the space-time evolution of the 127 distinct UPOs, the time-averaged mean and the variance of the spatiotemporal chaotic solution of KS equation Eq. (1) can be estimated. A simple averaging $< m(x) >_{\mathrm{UPO}}$ of all 127 mean patterns $m(x)$ for the UPOs yields the solid curve in Fig. 2(g), which should be compared with the dashed curve obtained by averaging an extensively chaotic field $u(t, x)$ over 10^6 time units. The relative error in the infinity norm between the patterns is 24% and is substantially better near the boundaries. Strikingly, $< m(x) >_{\mathrm{UPO}}$ has the same qualitative structure as the mean pattern of the attractor $< u(x) >$ using only a moderate number of low-period UPOs. In contrast, an average of the 127 variance patterns (solid line in Fig. 2(h)) does not agree as well (a relative error of 46%) with the variance of the extensively chaotic field $u(t, x)$ averaged over 10^6 time units but still reflects some of the qualitative features. These results

suggest that a knowledge of UPOs may help to understand the interesting mean patterns and localized dynamics observed recently in Faraday wave experiments [20].

Fig. 3 shows how the extent of localization and instability depends on the period T. To characterize the degree of localization of the UPOs, a localization number was defined as the fraction of the interval $[0, L]$ for which the variance $v(x)$ was smaller than 0.05 (the results were not sensitive to the choice of this cutoff). Fig. 3(a) shows the localization number versus the period T for all 127 UPOs. Although there is scatter in the points, we can draw a few conclusions: that UPOs with period less than about 8 don't exist; that shorter period UPOs are more strongly localized; and that there can be many UPOs of approximately the same period (say $T = 14$) and these can vary substantially in their localization. The outlier point with a localization of 0.6 for period $T = 30$ suggests that the right side of this curve is incomplete, that there are localized UPOs of higher period but our numerical algorithms were not able to find them. In Fig. 3(b), we summarize the instability of all 127 UPOs as a function of their period T. The instability of a UPO is defined as the sum $\sum_+ \lambda$ of all positive transverse Lyapunov exponents which are defined by $\lambda = \log(|m|)/T$, where m is a Floquet multiplier, i.e., an eigenvalue of the propagator matrix $\mathbf{M}_T$ in Eq. (3) evaluated for a UPO of period T [17]. Fig. 3(b) shows that, on average, smaller period UPOs are more unstable. Again the right side of this curve is incomplete and it would be interesting to extend the data using more sophisticated numerical algorithms.

Using the data in Fig. 3(b) one can estimate the fractal dimension D of the chaotic attractor. First, a fractal dimension is formerly associated with each UPO by generalizing the Kaplan-Yorke formula [17] to UPOs in terms of their transverse Lyapunov exponents; we find dimensions ranging from 6 to 12 for the 127 UPOs. The fractal dimension of the chaotic attractor can be viewed as an average over the fractal dimensions of the UPOs which are associated with the attractor. To obtain the fractal dimension over attractor, each UPO's dimension is summed with a weighting $1/(\sum_+ \lambda)$ (less unstable UPOs are weighted more heavily) which gives an estimate of $D = 9.0$ to the fractal dimension of the attractor. This is in good agreement with the Lyapunov fractal dimension $D = 8.8 \pm 0.1$ calculated directly

from the Lyapunov exponents of the spatiotemporal chaotic solution of Eq. (1) [15]. The convergence to the Lyapunov dimension of the estimate based on UPOs is statistical in that the error decreases approximately as $1/\sqrt{N}$ where N is the number of UPOs contributing to the weighted sum. Other weightings of the UPOs were tried [7, 21] but found not to give results as satisfactory as the $1/(\sum \lambda_+)$ weighting.

In conclusion, we have used an innovative numerical method to calculate for the first time many UPOs associated with a large high-dimensional pde, Eq. (1). An important numerical insight was the use of damping to increase the likelihood of convergence of an otherwise straightforward Newton method. Near-recurrences in the time-series data as long as 10^8 time units were found not to correspond to any computed UPOs. From the 127 distinct UPOs found using the damped-Newton method, we could estimate the fractal dimension of the attractor to be 9.0 ± 0.1 compared to the actual value of 8.8 ± 0.1. These UPOs were also used to predict successfully the qualitative features of the time-averaged mean pattern and the variance of the chaotic attractor. A new insight is that the UPOs are typically localized in space. This localization suggests a new way to think about the dynamically independent subsystems within extensive chaos. The localization also has important implications for the control of large chaotic systems using distributed sets of control points.

The present calculations raise two interesting questions for future work. One is to improve the numerical algorithms, primarily by using multishooting methods [22], so that UPOs of partial differential equations in two- and three-space dimensions can be calculated. It will then be quite interesting to determine whether there are systematic patterns of defects associated with UPOs as their period increases from their smallest value. The second question is to understand the implications of localized UPOs for spatially distributed control, e.g., by the OGY or delayed-feedback methods.

REFERENCES

*   Also Center for Nonlinear and Complex Systems, Duke U., Durham, NC

†   E-mail: zoldi@phy.duke.edu

[1] R. Artuso, E. Aurell, and P. Cvitanović, Nonlinearity **3**, 325 (1990).

[2] A. Politi and A. Torcini, Phys. Rev. Lett. **69**, 3421 (1992); A. Politi and A. Torcini, Chaos **2**, (293) (1992).

[3] R. Badii *et al.*, Rev. Mod. Phys. **66**, 1389 (1994).

[4] D. Pierson and F. Moss, Phys. Rev. Lett. **75**, 2124 (1995).

[5] M. Ding *et al.*, Phys. Rev. E **53**, 4334 (1996).

[6] J. Guckenheimer and P. Holmes, *Nonlinear Oscillations, Dynamical Systems, and Bifurcations of Vector Fields* (Springer-Verlag, New York, 1983).

[7] K. Pawelzik and H. G. Schuster, Phys. Rev. A **43**, 1808 (1991).

[8] E. Ott, C. Grebogi, and J. A. Yorke, Phys. Rev. Lett. **64**, 1196 (1990); K. Pyragas, Phys. Lett. A **170**, 421 (1992); G. Chen and X. Dong, Int. J. Bifurcation and Chaos **3**, 1363 (1993).

[9] M. C. Cross and P. C. Hohenberg, Rev. Mod. Phys. **65**, 851 (1993).

[10] H. S. Greenside, in *Semi-Analytic Methods for the Navier Stokes Equations*, *Proceedings of the CRM Workshop*, edited by K. Coughlin (Centre de Recherches Mathematiques, Montreal, Canada, 1997), in press; LANL chao-dyn/9612004.

[11] J. P. Crutchfield and K. Kaneko, Phys. Rev. Lett. **60**, 2715 (1988); Y.-C. Lai and R. L. Winslow, Phys. Rev. Lett. **74**, 5208 (1995).

[12] I. Aranson, H. Levine, and L. Tsimring, Phys. Rev. Lett. **72**, 2561 (1994); D. Auerbach and J. A. Yorke, J. Opt. Soc. Am. B **13**, 2178 (1996); M. E. Bleich, D. Hochheiser, J. V.

Moloney, and J. E. S. Socolar, Phys. Rev. E, **55** (3) 2119 (1997).

[13] In previous work, Politi et al [2] have studied UPOs of a 1d extensively chaotic system with *discrete* time, consisting of up to six weakly coupled Hénon maps. In contrast, our analysis concerns a continuous-time strongly-coupled system with an emphasis on the spatial structure of the UPOs.

[14] J. E. Dennis and R. Schnabel, *Numerical Methods for Unconstrained Optimization and Nonlinear Equations* (Prentice-Hall, Englewood Cliffs, NJ, 1983).

[15] P. Manneville, in *Macroscopic modeling of turbulent flows*, Vol. 230 of *Lecture Notes in Physics*, edited by O. Pironneau (Springer-Verlag, New York, 1985), pp. 319–326.

[16] Recently, F. Christiansen, P. Cvitanović and V. Putkaradze [Nonlinearity **10** 55 (1997)] also studied the KS equation to investigate how a chaotic attractor may be related to the UPOs whose closure defines that attractor. Their emphasis and results differ substantially from ours in that these authors considered a smaller *periodic* domain for which the chaotic dynamics is low-dimensional (we estimate $D \approx 2.2$ from their data) and for which the set of UPOs has an explicit symbolic dynamics.

[17] T. S. Parker and L. O. Chua, *Practical Numerical Algorithms for Chaotic Systems* (Springer-Verlag, New York, 1989).

[18] Our inability to find approximate recurrences from numerical output $\mathbf{U}(t)$ suggests that some of the widely used control methods [8] will not succeed in stabilizing UPOs since they depend crucially on knowing an approximate recurrence as input to the algorithm.

[19] UPOs are distinct in that their time-averaged pattern $m(x)$ and variance $v(x)$ averaged over one period, $m(x) = \langle u(t,x) \rangle$ and $v(x) = \langle (u(t,x) - m(x))^2 \rangle$ differed by at least 0.01 and their periods differed by at least 0.01.

[20] B. J. Gluckman, C. B. Arnold, and J. P. Gollub, Phys. Rev. E **51**, 1128 (1995); A. Kudrolli and J. P. Gollub, Physica D **97**, 133 (1996).

[21] C. Grebogi, E. Ott, and J. A. Yorke, Phys. Rev. A **37**, 1711 (1988).

[22] U. M. Ascher, R. M. M. Mattheij, and R. D. Russell, *Numerical Solution of Boundary Value Problems for Ordinary Differential Equations* (SIAM, Philadelphia, 1995).

FIGURES

FIG. 1.   Density plots of three representative UPOs $u(t, x)$ calculated by applying a damped-Newton method to the Kuramoto-Sivashinsky equation Eq. (1) in a spatial domain of length $L = 50$. The horizontal axis is space and the vertical axis spans a time interval of 35 time units. **(a)** A UPO of period $T = 9.9$ with dynamics localized near the right boundary; **(b)** A UPO of period $T = 10.7$ with dynamics localized in interior of the interval; **(c)** An extended UPO of period $T = 23.4$. The greyscales represent amplitude variations between about 3 and -3.

FIG. 2.   Time-averaged mean patterns $m(x) = < u(x, t) >$ and variance patterns $v(x) = < (u(x, t) - m(x))^2 >$ for the three representative UPOs of Fig. 1. **(a)** and **(b)**: for the UPO with dynamics localized near a boundary. **(c)** and **(d)**: for the UPO with dynamics localized away from boundaries. **(e)** and **(f)**: for the extended UPO. **(g)** and **(h)**: mean and variance patterns (solid lines) averaged over all 127 distinct UPOs. For comparison, the dashed lines give the corresponding mean and variance patterns obtained from an integration of a chaotic solution over 10^6 time units.

FIG. 3.   **(a)** Localization (fraction of the spatial domain that has variance $v(x)$ below 0.05) versus period T of 127 distinct UPOs calculated for the KS equation (Eq. (1)) in an extensively chaotic regime with system size $L = 50$. **(b)** Degree of instability as measured by the sum $\sum_+ \lambda$ of positive transverse Lyapunov exponents versus the period T for all 127 UPOs.
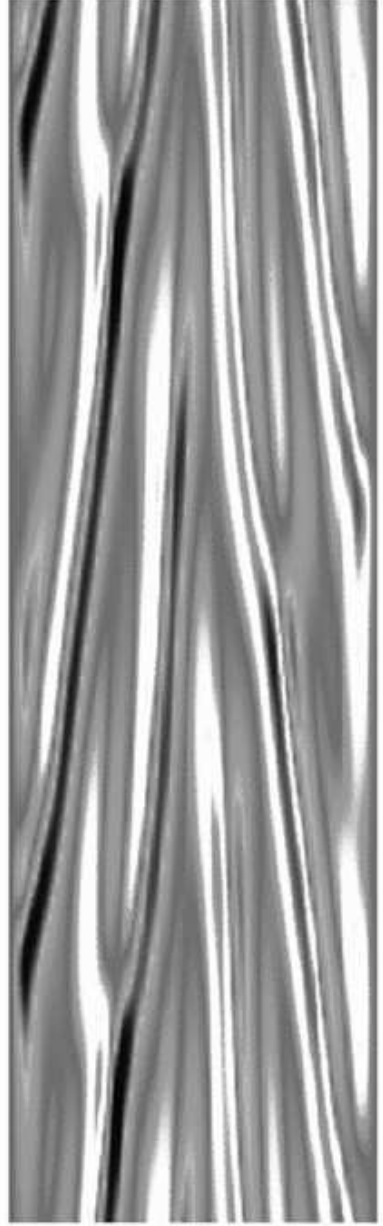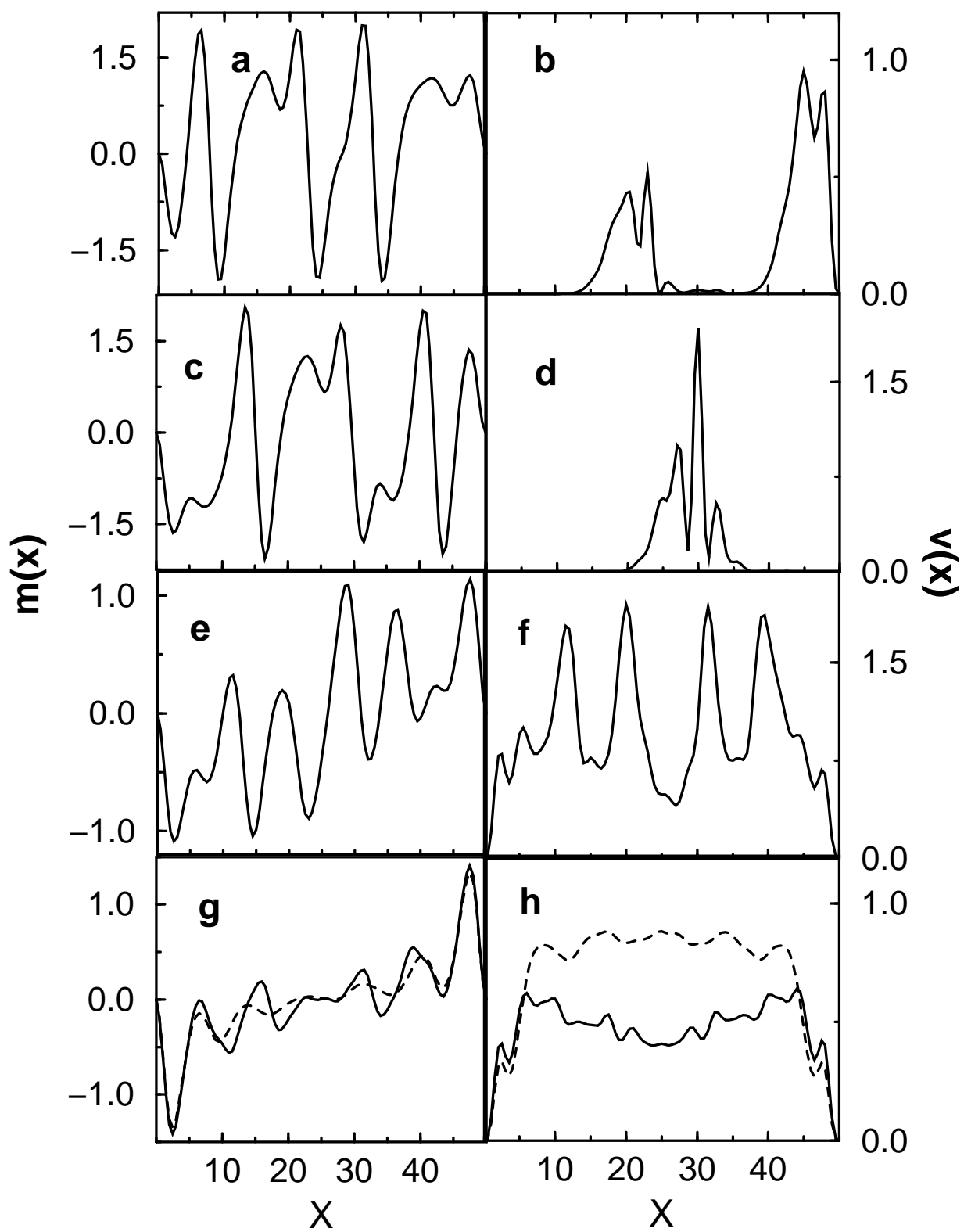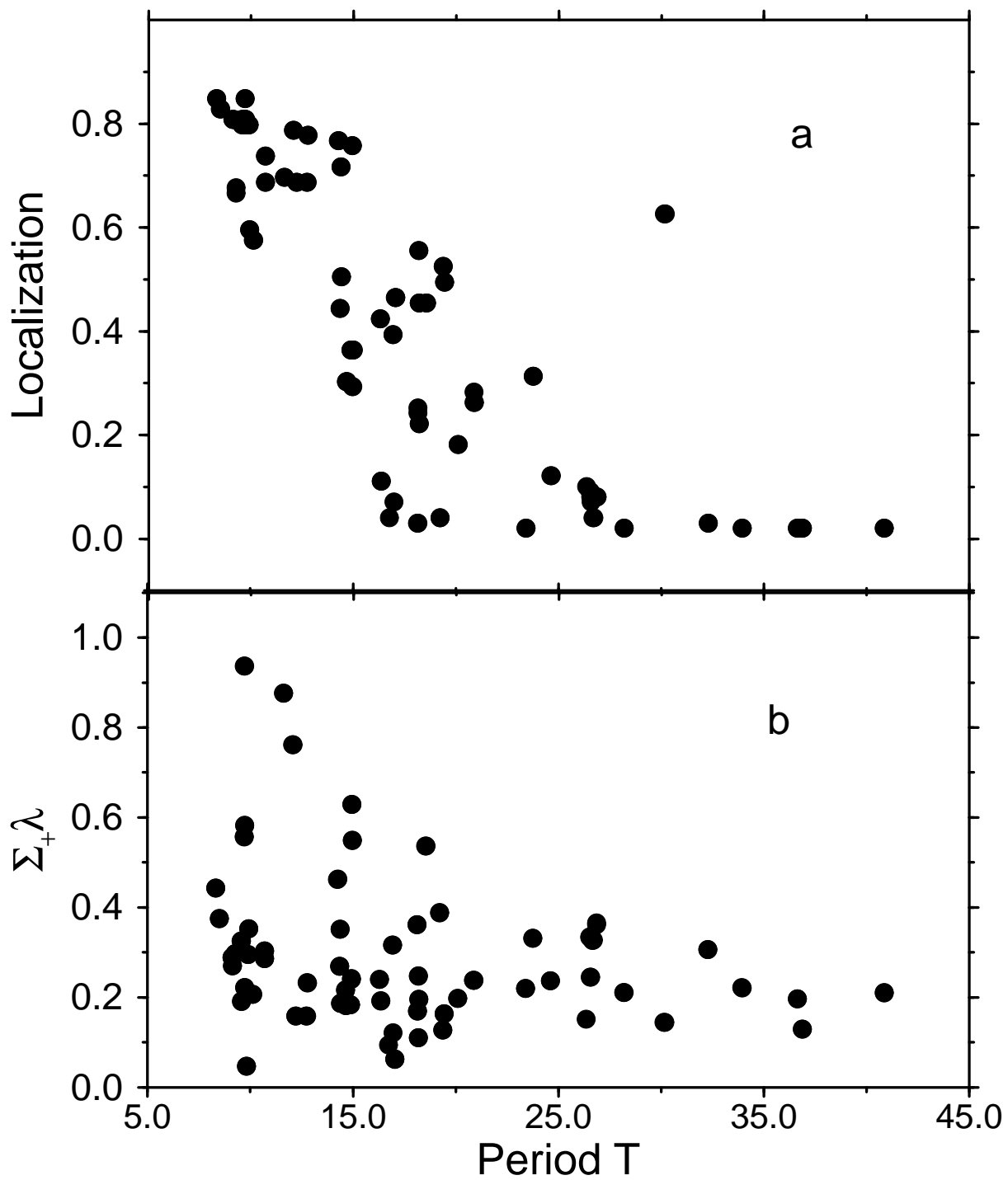
A   B   C

Fig 1 Zoldi and Greenside

Zoldi and Greenside Fig2

15

Fig 3 Zoldi and Greenside